A Simple Ekman-Type Model for Predicting Thermocline Displacement in the Tropical Pacific

P. WEBB DEWITT AND ANTS LEETMAA

Atlantic Oceanographic and Meteorological Laboratories, NOAA, Miami, FL 33149

(Manuscript received 25 July 1977, in final form 14 April 1978)

ABSTRACT

A linear model is developed for the near-equatorial zone to estimate wind-driven convergences in the near-surface viscous boundary layer. Using the winds observed during EASTROPAC, an attempt is made to relate these convergences to the measured displacements of the tropical thermocline. Between 4° and 15°N, the sign of the displacements is predicted; however, the amplitude is generally underestimated. At the equator, extremely large values of the vertical eddy coefficients are necessary in order to obtain agreement between predicted and observed changes. This probably indicates that some essential physics has been neglected.

1. Introduction

In a recent paper, Meyers (1975) examines the relationship between the seasonal variations in the Pacific North Equatorial Current and the wind field. He finds that between 10° and 25°N, most of the temporal variations in the meridional slope of the thermocline could be accounted for by meridional variations in the Ekman pumping. The latter is the vertical velocity that results from the divergence of the horizontal Ekman transport after the mean annual divergence is subtracted out. It is somewhat surprising that such a model should work so well. After all, fluctuating winds of these frequencies should generate baroclinic and barotropic Rossby waves.

Some insight as to why the model possibly works can be obtained from the paper of Anderson and Gill (1975). They consider an initial value problem in which a midlatitude ocean is spun up from rest. The initial mid-ocean response in their model is the Ekman pumping response. This continues until Rossby waves from the eastern boundary arrive, and then a steady Sverdrup balance is obtained. Near the equator a similar situation occurs, except that it is the Kelvin wave that propagates in from the west that stops the initial Ekman pumping response (Moore and Philander, 1977). However, if these waves are eliminated or strongly modified by dissipation, nonlinearities, bottom topography or vertical shear in the horizontal currents, then the local response might dominate.

As evidence against this, White (1977) presented a model for the response of the tropical North Pacific Ocean to wind forcing at the annual period. He found that the response consisted of a locally forced component (as did Meyers) and the baroclinic long waves that propagate in from the eastern boundary. The overall amplitude of the response was determined by the amplitude of the local response. White analyzed the bathythermograph (BT) data files for the entire North Pacific Ocean and appeared to find evidence for the baroclinic long waves, which he calculated to propagate zonally at a phase speed of 40 cm s^{-1} at 11°N and 15 cm s^{-1} at 18°N. In this model, the applied stress was assumed to be independent of longitude.

An examination of the wind stress curl computations of Wyrtki and Meyers (1975) for the tropical Pacific shows a zonal structure to the curl which appears to propagate to the west. The propagation speeds are those that White deduced from the BT data. Thus, in our opinion, there is some question as to whether the presence of the Rossby waves has been demonstrated. With this in mind, an attempt is made to extend the Ekman pumping analysis to the equator. Within a couple of degrees of the equator, the time response of the ocean is extremely rapid (Moore and Philander, 1977). In addition to Rossby waves, Kelvin and Yanai waves are also present. Furthermore, the simple Ekman dynamics that applies in higher latitudes must break down (Robinson, 1966). Most likely nonlinear effects become important. However, these are not tractable in a simple model. Thus the model considered is linear and viscous with the understanding that in the proximity of the equator the physic is probably incorrectly modeled, and that the vertical eddy coefficient might have to be varied as a reflection of this inadequacy.

2. Model formulation

The near-surface layer of the tropical oceans is characterized by a relatively thick [O(100 m)], quasi-homogeneous upper layer, beneath which the temperature very rapidly falls to its deep-water value. We are concerned with predicting changes in thickness of this upper layer. A two-layer ocean is considered with an upper homogeneous layer of depth D[O(100 m)]. Viscous effects are assumed to be confined to this layer. Away from the equator, the Ekman depth might be less than D; close to the equator, viscous effects are important throughout D. At the sea surface a wind stress is applied, and at the bottom of this layer it is assumed that the horizontal frictional velocities go to zero. There can, however, be a vertical velocity at this level which results from frictional convergences throughout the whole layer. This causes the lower interface to move up or down. In the model considered, the mean annual Ekman convergence is subtracted out. Away from the equator, this is balanced in the mean by geostrophic convergence, i.e., the Sverdrup balance holds. The model is concerned not with the mean state, but with fluctuations about this state.

We consider an ocean with an upper homogeneous layer of depth D that is unbounded in the horizontal direction. The coordinate x is positive eastward, y positive northward and z positive upward. The origin is at the sea surface. The respective velocity components are u, v and w. Horizontal pressure gradients are ignored. This is not to say that they are unimportant. Studies have shown that in the *mean* state, the east-west wind stress balances the vertically integrated zonal pressure gradient (Katz, 1977). It is assumed that in this model the pressure gradients are not important in the dynamics of the frictional boundary layer (this is the usual assumption in Ekman-layer theory). However, the frictional convergences do redistribute the mass in the upper ocean and thereby create pressure gradients. These in turn are balanced away from the equator by geostrophic velocities. In this paper there is no discussion about these geostrophic velocities. The motion is also assumed to occur on a time scale longer than that required to set up the frictional boundary layer. Under these assumptions the equations of motion are

$$fu = \gamma v_{zz}, \quad -fv = \gamma u_{zz}, \quad u_x = \frac{\partial u}{\partial x}, \quad \text{etc.,} \tag{1}$$

where $f = 2\Omega \sin\phi$ is the Coriolis parameter and γ is the vertical eddy viscosity.

The boundary conditions are

$$\left.\begin{aligned} u_z = \tau^x/\gamma; \quad v_z = \tau^y/\gamma \quad &(\text{at} \quad z = 0) \\ u = v = 0 \quad &(\text{at} \quad z = -D) \end{aligned}\right\}, \tag{2}$$

where τ^x and τ^y are the horizontal components of wind stress at the sea surface. Vanishing of the horizontal velocities at the base of the mixed layer applies only to the frictional velocities. The geostrophic velocities probably do not vanish.

As in classical theory (Ekman, 1905), the solutions to (1) are assumed to be of the form

$$\left.\begin{aligned} u &= Ae^{kz}[\cos(kz + C_1)] + Be^{-kz}[\cos(kz + C_2)] \\ v &= Ae^{kz}[\sin(kz + C_1)] - Be^{-kz}[\sin(kz + C_2)] \end{aligned}\right\}, \tag{3}$$

where A, B, C_1 and C_2 are constants; and

$$k = (f/2\gamma)^{1/2}.$$

After solving for A, B, C_1 and C_2, the solutions for u and v are

$$\left.\begin{aligned} u = (2k\gamma)^{-1} &\left[(\tau^x + \tau^y)(\sinh kz)(\cos kz) + (\tau^x - \tau^y)(\cosh kz)(\sin kz) \right.\right. \\ &\left.\left. + (M\tau^x + N\tau^y)(\cosh kz)(\cos kz) + (N\tau^x - M\tau^y)(\sinh kz)(\sin kz)\right] \\ v = (2k\gamma)^{-1} &\left[(\tau^x + \tau^y)(\cosh kz)(\sin kz) - (\tau^x - \tau^y)(\sinh kz)(\cos kz) \right.\right. \\ &\left.\left. + (M\tau^x + N\tau^y)(\sinh kz)(\sin kz) - (N\tau^x - M\tau^y)(\cosh kz)(\cos kz)\right] \end{aligned}\right\}, \tag{4}$$

where

$$M = \frac{\sinh 2kD + \sin 2kD}{\cosh 2kD + \cos 2kD}, \qquad N = \frac{\sinh 2kD - \sin 2kD}{\cosh 2kD + \cos 2kD}.$$

With the boundary condition $(w)_{z=0} = 0$, the continuity equation

$$u_x + v_y + w_z = 0 \tag{5}$$

can be vertically integrated from $z = 0$ to $z = -D$, i.e.,

$$w_{-D} = \int_{-D}^{0} (u_x + v_y)dz. \tag{6}$$

Inserting (4) into (6), performing the indicated differentiation and integration with the further assumption that $f \approx \beta y$, the following solution for Ekman pumping is obtained:

$$w_{-D} = \left(\frac{2}{\beta y}\right)\left[\begin{array}{l}(\tau_x^x + \tau_y^y)\left(\dfrac{\sinh kD \sin kD}{\cosh 2kD + \cos 2kD}\right) \\ + (\tau_x^y - \tau_y^x)\left(\dfrac{1}{2} - \dfrac{\cosh kD \cos kD}{\cosh 2kD + \cos 2kD}\right)\end{array}\right]$$

$$+ \left(\frac{2}{\beta y^2}\right)\left[\tau^x\left(\frac{1}{2} - \frac{\cosh kD \cos kD}{\cosh 2kD + \cos 2kD}\right) - \tau^y\left(\frac{\sinh kD \sin kD}{\cosh 2kD + \cos 2kD}\right)\right]$$

$$+ \left(\frac{\tau^x D}{\gamma k y}\right)\left[\begin{array}{l}\sin kD \cos^2 kD \cosh kD \\ \quad - \cos kD \sinh kD \cosh^2 kD \\ \quad - \sin^2 kD \cos kD \sinh kD \\ \quad - \sin kD \sinh^2 kD \cosh kD\end{array}\right](\cosh 2kD + \cos 2kD)^{-2}$$

$$+ \left(\frac{\tau^y D}{\gamma k Y}\right)\left[\begin{array}{l}\sin kD \cos^2 kD \cosh kD \\ \quad + \cos kD \sinh kD \cosh^2 kD \\ \quad + \sin^2 kD \cos kD \sinh kD \\ \quad - \sin kD \sinh^2 kD \cosh kD\end{array}\right](\cosh 2kD + \cos 2kD)^{-2}, \quad (7)$$

where

$$k = \left(\frac{\beta y}{2\gamma}\right)^{1/2}$$

and terms containing D_x and D_y are neglected as they can be shown to be small. Asymptotic forms of Eq. (7) turn out to be useful. Near the equator (limit $kD \to 0$), (7) reduces to

$$w_{-D} = \frac{D^2}{2\gamma}(\tau_x^x + \tau_y^y) - \frac{5}{24}\frac{D^4\beta}{\gamma^2}\tau^x. \quad (8)$$

The product kD may be written as $kD = \pi(D/D_E)$, where D_E is the classical ideal Ekman depth as given by

$$D_E = \pi(2\gamma/f)^{1/2}. \quad (9)$$

When the Ekman depth is small compared to the depth of the mixed-layer ($kD \gg \pi$), Eq. (7) reduces to

$$w_{-D} \approx \left(\frac{1}{\beta y}\right)(\tau_x^y - \tau_y^x) + \left(\frac{1}{\beta y^2}\right)\tau^x. \quad (10)$$

Computations of (4) and (7) were made on a Hewlett-Packard 9815-A programable calculator.

In classical Ekman theory for a finite-depth ocean (Ekman, 1905), the nature of the flow is governed by the ratio of the ocean depth H to the ideal Ekman depth D_E [Eq. (9)]. When the ratio $H/D_E \leq 0.1$, the resultant flow is couette-like and the velocity profile is approximately linear in z. As the ratio increases, the classical Ekman spiral emerges.

The u and v fields as given by (4) adhere to the classical Ekman flow for a finite depth (Fig. 1). For discussion purposes, the Ekman pumping model will be divided into three regimes: the regime near the equator where the resultant flow is couette-like, the regime far away from the equator where the classical Ekman spiral is found, and the transition zone between these two regimes.

3. Model results

a. East-west wind stress

Before using observed wind stress data, several examples are shown using ideal stresses to demon-

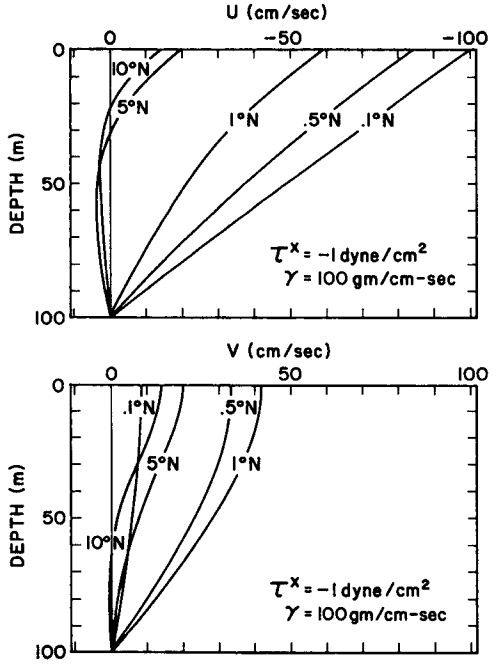

FIG. 1. The horizontal velocity field as computed by Eq. (4) for various latitudes with $D = 100$ m, $\tau^x = -1$ dyn cm^{-2} and $\tau^y = 0$.

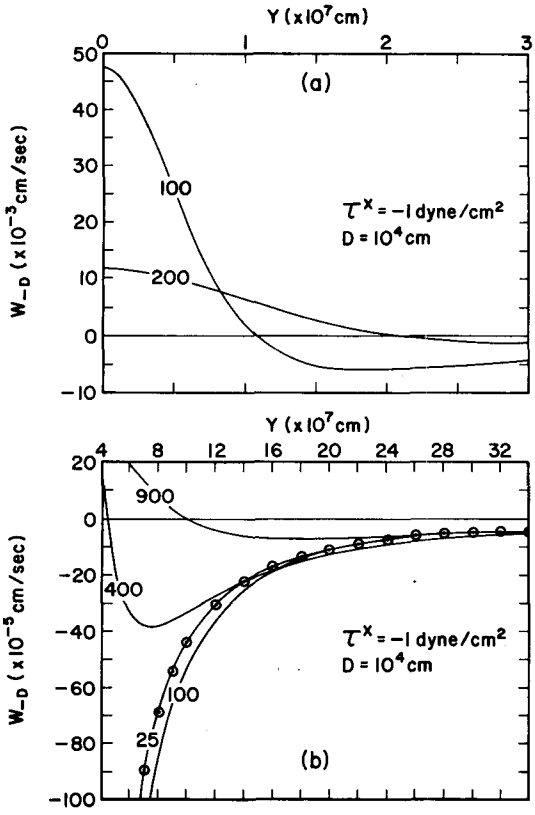

FIG. 2. Vertical velocity (w_{-D}) within 300 km of the equator (a) as computed by (7) for various eddy viscosities (g cm^{-1} s^{-1}) as a function of y, with $\tau^x = -1$ dyn cm^{-2}, and vertical velocity beyond 400 km of the equator (b). The circled points were computed using Eq. (10).

strate the properties of (7). For a constant wind stress from the east ($\tau^x = -1$ dyn cm^{-2}), Eq. (7) indicates a strong divergence (positive w_{-D}) in the couette regime (Fig. 2a). Proceeding northward, the w_{-D} field becomes convergent (negative w_{-D}) as the Ekman spiral regime is encountered. The divergence at the equator is proportional to the inverse square of the eddy viscosity [Eq. (8)], whereas the width of the divergence region is directly proportional to the eddy viscosity.

Fig. 2b indicates the w_{-D} fields for various eddy viscosities. As y increases, the w_{-D} fields approach the ideal Ekman solution as given by Eq. (10). For a particular eddy viscosity and with $y \geq (\gamma/5) \times 10^7$ cm, the values of w_{-D} as computed by (7) and (10) are within 5% of each other.

b. *North-south wind stress*

A constant wind stress from the south ($\tau^y = 1$ dyn cm^{-2}) produces the w_{-D} field shown in Fig. 3a. At the equator, w_{-D} is zero [Eq. (8)]. Proceeding northward, a very strong convergence is predicted in the transition zone between the couette and Ekman regimes. The maximum vertical velocity of the convergence is proportional to the inverse square of the eddy viscosity. The northward location of the maximum convergence is directly proportional to the eddy viscosity. The vertical velocity field south of the equator is the negative of that shown, i.e., there is a strong divergence. A qualitative description of the preceeding is to be found in Cromwell (1953).

The w_{-D} field for various eddy viscosities is shown in Fig. 3b. When D_E for a particular γ becomes less than D, a divergence occurs as shown by the $\gamma = 25$ curve for $y > 3 \times 10^7$ cm.

c. *The wind stress curl and gradient*

Fig. 4 is presented to illustrate the relative importance of each term in Eq. (7). The stress derivative terms are assumed to have a magnitude of 10^{-8} dyn cm^{-3}, while the stress terms are assigned a value of 0.1 dyn cm^{-2}. These are typical values for the tropics. At the equator, the contribution from the wind stress curl terms is zero, whereas the wind stress gradient terms produce a vertical velocity as given by Eq. (8). Proceeding northward, the wind stress gradient terms become increasingly less important, while the wind stress curl terms go through a maximum, then slowly decrease in importance. In the Ekman spiral regime, the wind stress curl terms dominate, and the contribution

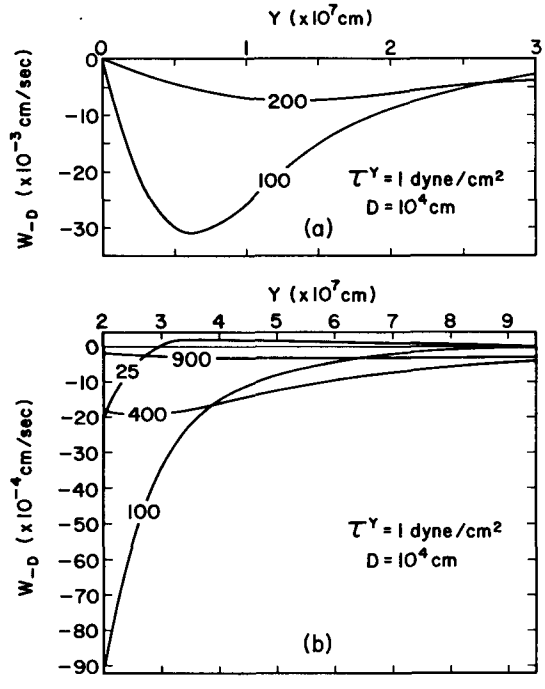

FIG. 3. Vertical velocity (w_{-D}) within 300 km of the equator (a) as computed by (7) for various eddy viscosities as a function of y, with $\tau^y = 1$ dyn cm^{-2}, and vertical velocity beyond 200 km of the equator (b).

from the wind stress gradient terms becomes insignificant.

4. Comparison with observed data

The ability of this model to reproduce fluctuations in the depth of the thermocline was examined along meridian 119°W, between 1° and 15°N. The effects of Ekman pumping at the equator were examined separately at 119° and 98°W.

During the EASTROPAC Experiment, a hydrographic section was taken approximately every two months along 119°W. The depth of the 20°C isotherm, as given in the EASTROPAC Atlases (Love, 1971, 1972a,b, 1973, 1975), was chosen to represent the top of the thermocline. Ekman pumping was used in an attempt to predict the depth fluctuations of this isotherm between consecutive surveys.

The necessary wind stresses for the model were obtained from the bimonthly average wind field charts presented in the EASTROPAC Atlases. From the bimonthly wind velocities, the annual mean wind velocities [as computed over 2° latitude × 10° longitude quadrangles for the experimental area by Wyrtki and Meyers (1975)] were subtracted out to eliminate the mean annual divergence of Ekman transport. The wind stresses were then determined using

$$\left.\begin{aligned}\tau^x &= \rho_a C W W_x \\ \tau^y &= \rho_a C W W_y\end{aligned}\right\}, \qquad (11)$$

where $\rho_a = 1.2$ kg m^{-3} is the density of the atmosphere, $C = 1.5 \times 10^{-2}$, and W is the wind speed in meters per second (Malkus, 1962; Wyrtki and Meyers, 1975).

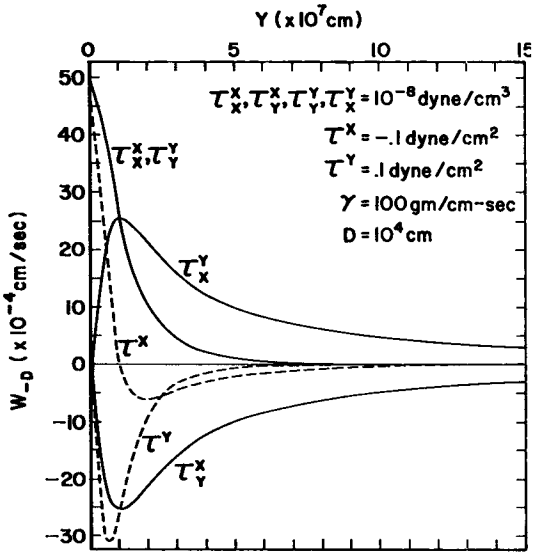

FIG. 4. The relative effects of the various wind stresses on the w_{-D} field (7) as a function of y.

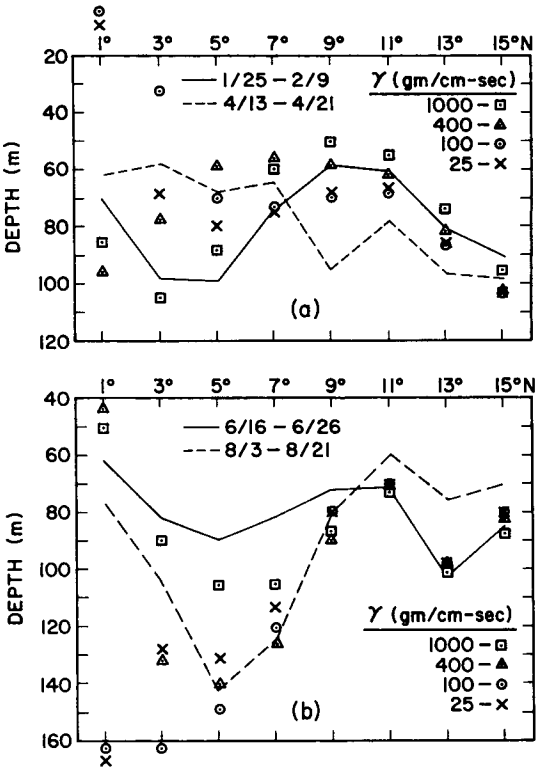

FIG. 5. Comparison between the actual depth fluctuations during the EASTROPAC Experiment of the 20°C isotherm along meridian 119°W, and the predicted depth fluctuations as computed for various eddy viscosities by Eq. (12). The model depth D was chosen to be 100 m. See text for further explanation.

Assuming that the calculated wind stresses were constant over the bi-monthly wind periods, the predicted depth of the 20°C isotherm was determined using

$$z = \int_{t_0}^{t} w_{-D}\,dt + z_0, \qquad (12)$$

where z_0 is the depth of the isotherm at the initial time t_0. The model depth D was chosen to be 10^4 cm. This is approximately the mean depth of the 20°C isotherm.

a. Ekman pumping along 119° W

Fig. 5 presents the comparison between the predicted thermocline topography for various eddy coefficients and the actual depth fluctuations of the 20°C isotherm. The initial topography of the 20°C isotherm is shown by the solid line; the one several months later is shown by the dashed line; i.e., it is the dashed line that we are attempting to predict.

At 1°N the smaller eddy coefficients (25, 100) greatly overestimate the thermocline displacements in both cases, whereas the larger coefficients (400, 1000) predict movement of more reasonable amplitude in the wrong direction.

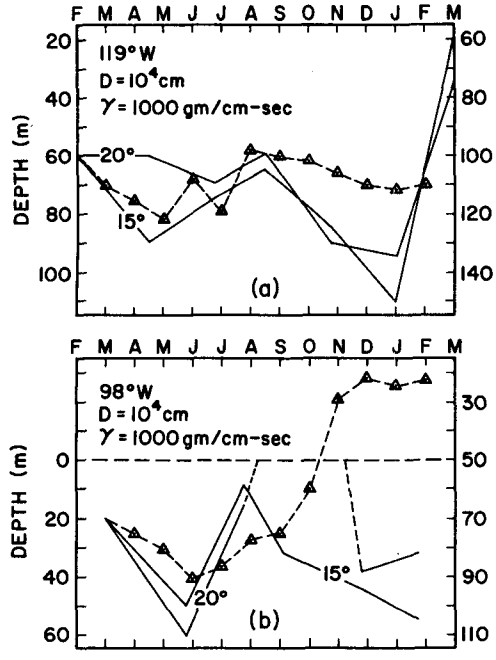

FIG. 6. Comparison between the actual depth fluctuations at the equator (February 1967–March 1968) of the 20°C and 15°C isotherms, and the predicted depth fluctuations as given by Eq. (12). The depth of the 20°C isotherm is given on the left-hand side of the graph, while the depth of the 15°C isotherm is given on the right-hand side. See text for further explanation.

In Fig. 5a, the eddy coefficients of 25 and 100 produce better predictions north of 9°N. However, the magnitudes of the downward predictions are approximately one-half of the actual deepening of the 20°C isotherm. At 5°N, good predictions occurred with $\gamma = 25, 100, 400$. In general the smaller eddy coefficients predict the correct sign for the displacements and reasonable magnitudes.

In Fig. 5b, the very strong deepening of the isotherm between 4° and 9°N is again well predicted. North of 9°N, the direction of movement is correctly ascertained. However, the calculated magnitude of movement is at best a third of the actual movement.

It seems that the model provides reasonable results from about 4° to 15°N. In this region, the midlatitude Ekman solution is still a close approximation to the total solution given by (7). In both Figs. 5a and 5b there appears to be a general underestimation in the calculated magnitude of movement north of 9°N. This discrepancy may be the result of underestimating the wind stress and its curl. Evidence for this comes from Meyers (1975). He predicts extremely well the seasonal depth cycle of the thermocline at 10°N and 155°W using essentially Eq. (10). In that area the winds are steadier and there is more ship traffic providing wind data. Thus, better estimates can be made of the curl.

From 1° to 4°N none of the solutions seem to do a very good job. This is the transition region from the Ekman spiral solution to the couette solution.

It should be noted that the functional dependence of Eq. (7) on the magnitude of the eddy coefficient γ is somewhat complicated (Figs. 5a and 5b). This dependence is better visualized in Figs. 2a and 2b, 3a and 3b with regards to the shifting of the relative positions of the ideal curves for various eddy viscosities.

b. Ekman pumping along the equator

To test (7) [or its asynoptotic limit (8)] at the equator, the depth fluctuations of the 20 and 15°C isotherms, as reported during the EASTROPAC Experiment at 119° and 98°W, were utilized. The necessary wind stresses were computed as in the previous section except that monthly mean wind velocities [as computed during the experiment for 2° latitude × 10° longitude quadrangles (Wyrtki and Meyers, 1975)] were employed instead of the bimonthly winds as reported in the EASTROPAC Atlases. The eddy viscosity used was 1000 g cm^{-1} s^{-1} and the depth D was 10^4 cm. The higher eddy viscosity was necessary in order to obtain reasonable values for the Ekman pumping. As before, the prediction of the thermocline depth was made using (12).

At 119°W (Fig. 6a), the model predicts fairly well the direction of movement of the 15°C isotherm until about August. From that time on, the predicted magnitude of movement is not large enough to match the observed depth changes. At 98°W, the depth changes as predicted coincide well, again until August, with the observed depth changes of the 20 and 15°C isotherms. During September, the observed 20°C isotherm breaks the surface while the 15°C isotherm deepens appreciably with respect to the preceeding observation period. The model during this time does predict a strong divergence—strong enough to cause the isotherms to break the surface.

5. Discussion

It should be emphasized that the main drawback in doing this comparison was the difficulty in estimating the spatial distribution of the wind stress. In our opinion the quantity and quality of the available data were marginal. Nevertheless, between 4° and 15°N, reasonable agreement was obtained between the predicted thermocline displacements and the observed displacements, both in terms of the magnitude of the displacement and the direction. North of 4°N the results of our more complicated solution were quite well reproduced by the simpler midlatitude Ekman solution [Eq. (10)].

This indicated that the more complicated formalism in this region is unnecessary and that the solution is more nearly independent of the eddy coefficients.

At the equator there was limited agreement between the model and the observations. These results perhaps should not be taken too seriously because the flow in this region is probably nonlinear. The thermal structure indicated that the Equatorial Undercurrent was present during most of the time period over which the comparison was made. The agreement does indicate, however, that the displacements are, perhaps, in some complicated way, related to the wind stress. Between the couette and Ekman spiral regimes, the agreement between the model and the observations was poor, and a more complicated dynamics must apply.

Horizontal pressure gradients are ignored in the present model. To reiterate, this is not to say that they are unimportant in the dynamics of the tropical oceans. The present model is intended not to be dynamically complete, but an attempt to model one aspect of a very complicated system, i.e., to see how well the redistribution of mass by Ekman pumping could account for thermocline displacements.

Acknowledgments. The authors are especially grateful to Drs. David Behringer and Robert Molinari for their comments and suggestions during the course of this study. Thanks are also due to Mr. Gary Meyers for making available the annual mean wind data for the study area.

REFERENCES

Anderson, D. L. T., and A. E. Gill, 1975: Spin-up of a stratified ocean, with applications to upwelling. *Deep-Sea Res.*, **22**, 583–596.

Cromwell, T., 1953: Circulation in a meridional plane in the central equatorial Pacific. *J. Mar. Res.*, **12**, 196–213.

Ekman, V. W., 1905: Om jordrotationens inverkan på vindstrommar i hafvet. *Nyt. Mag. Naturvid.*, **20**, Kristiania.

Katz, E. J., and collaborators, 1977: Zonal pressure gradient along the equatorial Atlantic. *J. Mar. Res.*, **35**, 293–307.

Love, C. M., Ed., 1971: *EASTROPAC Atlas*, Vol. 3. Circ. 330, Nat. Mar. Fish. Serv., Washington, DC.

———, 1972a: *EASTROPAC Atlas*, Vol. 1. Circ. 330, Nat. Mar. Fish. Serv., Washington, DC.

———, 1972b: *EASTROPAC Atlas*, Vol. 5. Circ. 330, Nat. Mar. Fish. Serv., Washington, DC.

———, 1973: *EASTROPAC Atlas*, Vol. 7. Circ. 330, Nat. Mar. Fish. Serv., Washington, DC.

———, 1975: *EASTROPAC Atlas*, Vol. 9. Circ. 330, Nat. Mar. Fish. Serv., Washington, DC.

Malkus, J. S., 1962: Large scale interactions. *The Sea*, Vol. 1, M. N. Hill, Ed., Interscience, 88–294.

Meyers, G., 1975: Seasonal variation in transport of the Pacific North Equatorial Current relative to the wind field. *J. Phys. Oceanogr.*, **5**, 442–449.

Moore, D. W. and S. G. H. Philander, 1977: Modeling of the tropical oceanic circulation. *The Sea*, Vol. 6, E. D. Goldberg, I. N. McCave, J. J. O'Brien and J. H. Steele, Eds., Interscience, 319–362.

Robinson, A. R., 1966: An investigation into the wind as the cause of Equatorial Undercurrent. *J. Mar. Res.*, **24**, 179–204.

White, W. B., 1977: Annual forcing of baroclinic long waves in the tropical North Pacific Ocean. *J. Phys. Oceanogr.*, **7**, 50–61.

Wyrtki, K., and G. Meyers, 1975: The trade wind field over the Pacific Ocean: Part I. The mean field and the mean annual variation. Hawaii Inst. Geophys., HIG-75-1, 67 pp.